Sol–Gel with Phase Separation. Hierarchically Porous Materials Optimized for High-Performance Liquid Chromatography Separations

KAZUKI NAKANISHI*,† AND NOBUO TANAKA‡

Department of Chemistry, Graduate School of Science, Kyoto University, Kitashirakawa, Sakyo-ku, Kyoto 606-8502, Japan, and Department of Biomolecular Engineering, Graduate School of Science and Technology, Kyoto Institute of Technology, Matsugasaki, Sakyo-ku, Kyoto 606-8585, Japan

Received November 29, 2006

ABSTRACT

Sol–gel processes for fabricating oxides or metalloxane polymers with controlled porous structures have been reviewed. Gel materials having controlled macropores are synthesized by polymerization-induced phase separation and concurrent sol–gel transition in a variety of chemical compositions. Several variations of tailoring mesopore structures within the macroporous materials are introduced, which enable one to design hierarchically porous metal oxide and metalloxane polymer materials. Applications of monolithic silica gels having hierarchical macro/mesoporous structure to the separation media of high-performance liquid chromatography, HPLC, are described.

1. Introduction

Fifteen years have past since the first systematic study of monolithic porous silica with controlled macropores via the sol–gel method accompanied by phase separation was reported.[1] Sol–gel oxide materials characterized by the well-defined macropores were out of any existing category of inorganic gels. They were, however, very similar in morphology to the porous glasses prepared via metastable phase separation in immiscible glass-forming oxide systems followed by selective leaching of one of the separated phases.[2] With regard to the morphology formation process as a competition between dynamics of polymerization-induced phase separation and steep chemical sol–gel transition, the dependence of macroporous morphology on various synthesis parameters has been consistently interpreted. The experimental system has been readily extended to organo-silicon and silica-based multicomponent oxide systems. It has been found only recently, however, that pure titanium, zirconium, and aluminum oxides with well-defined macropores can also be fabricated. It has been further found that irrespective of the kind of precursors, whether they are metal alkoxides, metal salts, or a colloidal dispersion of oxides, a common structure-formation process has been confirmed. In this Account, porous materials designed by a sol–gel process accompanied by phase separation are reviewed, using polysiloxane systems as major examples. Their application to monolithic high-performance liquid chromatography (HPLC) columns is described in the last part.

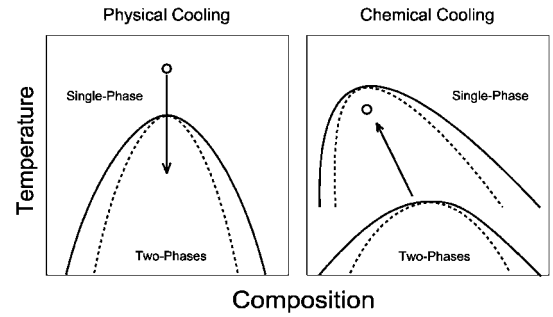

FIGURE 1. Schematic representations of physical vs chemical coolings.

2. Background and Principles

With the systems containing tetraalkoxysilane and appropriate additives as a starting point, the polymerization-induced phase separation, especially the spinodal decomposition, has been extensively utilized to generate well-defined heterogeneous structures.[3] Typical examples of applicable precursors and additive components are summarized in Tables 1 and 2, respectively. In most cases, the hydrolysis is conducted under acidic conditions where a relatively narrow distribution of growing oligomers can be obtained.[4] Although the polymerization reaction is conducted at a constant temperature, the phase separation is induced by the polymerization reaction itself.[5] The simplified free energy change of mixing multiple constituents in a solution, ΔG, can be written as

$$\Delta G = \Delta H - T\Delta S \quad (1)$$

When the sign of ΔG becomes positive, the thermodynamic driving force for phase separation is generated. The polymerization among any constituents usually reduces the ΔS term by decreasing the freedom in chemical configurations, whereas the physical cooling of the system is expressed by the reduction in T. In either case, the absolute value of the $T\Delta S$ term decreases and the phase separation is equivalently induced (Figure 1).[6] The po-

Kazuki Nakanishi is an associate professor in the Department of Chemistry, Graduate School of Science, Kyoto University, Kyoto, Japan. He graduated from the Faculty of Engineering, Kyoto University, and obtained his Doctor of Engineering degree from Kyoto University in 1991. He became interested in the competitive processes between phase separation and sol–gel transition in 1986 when he joined the Department of Material Chemistry, Graduate School of Engineering, Kyoto University, as a research associate. His research focuses on the sol–gel-based chemistry for integrated design of hierarchically porous materials in ceramics, organic–inorganic hybrids, and colloidal systems.

Nobuo Tanaka is a professor in the Department of Biomolecular Engineering, Graduate School of Science and Technology, Kyoto Institute of Technology, Kyoto, Japan. He has been continuously working on chromatography columns, stationary phases, separation mechanisms, and the separations of very closely related compounds, including isomers, isotopes, and enantiomers, since the 1970s. His current research interest includes the development of monolithic silica columns for various modes of HPLC that can attain a much higher level of performance than particle-packed columns in practical applications.

* Corresponding author.
† Kyoto University.
‡ Kyoto Institute of Technology.

10.1021/ar600034p CCC: $37.00
Published on Web 07/26/2007

Table 1. Precursors and Their Variations of Sol–Gel Systems Accompanied by Phase Separation

general classification	precursor type/ applicable element	possible variations	possible combinations	refs
tetrafunctional alkoxide	Si, Ti, Zr, Al-alkoxide	$Si(OMe)_4$, $Si(OEt)_4$, $Ti(O\text{-}i\text{-}Pr)_4$, $Ti(O\text{-}n\text{-}Pr)_4$, $Zr(O\text{-}i\text{-}Pr)_4$, $Al(O\text{-}sec\text{-}Bu)_3$	Si-Ti, Si-Zr, Si-Al, Si-colloidal particles	1, 3, 8, 10, 19–21
trifunctional alkoxide	alkyltrialkoxysilane	$RSi(OR')_3$, $R_2Si(OR')_2$	R = methyl, ethyl, vinyl, allyl, and others; R′ = methyl or ethyl	9
bridged alkoxide	bis(trialkoxysilyl)alkane	$(R'O)_3SiRSi(OR')_3$	R = methylene, ethylene, propylene, diethylbenzene, and others; R′ = methyl or ethyl	9, 33
colloidal dispersion	silica, titania	acid or base stabilized		14
polysilicate solution	water glass (alkaline silicate)	–		13
metal salt	aluminum chloride/ nitrate	iron(III), chromium(III)	additions of yttrium salt for YAG, magnesium salt for spinel; doping rare earth salts for luminescent properties	12

Table 2. Reaction Conditions, Additives, and Phase Relations in Various Systems

precursor	hydrolysis/ polycondensation conditions	additives (except water)	gel phase	fluid phase	refs
tetraalkoxysilane	water/Si < 2	polar solvent	siloxane	solvent mixture	3, 8
alkyltrialkoxysilane	water/Si < 3	alcohols	siloxane	solvent mixture	9
bis(trialkoxysilyl)alkane	water/Si > 10	none	siloxane	solvent mixture	9, 33
tetraalkoxysilane	water/Si > 4	strongly hydrogen bonding polymer, nonionic surfactant, cationic surfactant	siloxane with polymer	solvent mixture	3, 19–21
tetraalkoxysilane	water/Si > 4	weakly hydrogen bonding polymer, anionic surfactant	siloxane	solvent mixture with polymer	1
water glass	destabilization by acid	weakly hydrogen bonding polymer, anionic surfactant	polysilicate	solvent mixture with polymer	13
titania colloid	destabilization by base	strongly hydrogen bonding polymer	titanoxane with polymer	solvent mixture	14
titanium alkoxide	water/Si > 4		titanoxane with polymer	solvent mixture	10
zirconium alkoxide	water/Si > 4		zirconoxane with polymer	solvent mixture	unpublished
aluminum chloride	water/Si > 4	strongly hydrogen bonding polymer	aluminoxane	solvent mixture with polymer	12

lymerization can be regarded as a "chemical cooling" process in this respect. In practice, poor solvents of the oligomers, several kinds of water-soluble polymers, and surfactants can be used as an inducer of the phase separation driven by the polymerization reaction.

Sol–gel systems depicted here undergo a phase separation to generate micrometer-range heterogeneity composed of gel and fluid phases. After the solidification (gelation) of the whole system, the fluid phase can be removed relatively easily to leave pore spaces on the length scale of micrometers. In many cases of thermally induced phase separation in metallic alloys, polymer blends, and multicomponent glasses, the kinetics of phase separation can be externally controlled through temperature. One can quench the shape and size of the developing phase domains simply by cooling the system. On the other hand, the structure formation process has a more or less spontaneous nature in the present sol–gel systems. Both the onset of phase separation and sol–gel transition are governed by the kinetics of chemical bond formation. With a predetermined composition, the homogeneously dissolved starting constituents are just left to react at a constant temperature in a closed condition (to avoid evaporation of volatile components). As shown in Tables 1 and 2, it is noteworthy that not a few gel-forming systems exhibit common features of concurrent phase separation and sol–gel transition, irrespective of the difference in the origins of their gel-forming reactions.

When the phase separation is induced in the unstable region of a phase diagram (a temperature-composition region within the spinodal curve), a specific process called spinodal decomposition occurs. With comparable volume fractions of conjugate phase domains without crystallographic or mechanical anisotropy, a spongelike structure called a co-continuous structure forms (Figure 2, top). The co-continuous structure is characterized by mutually continuous conjugate domains and hyperbolic interfaces.

The final morphology of the spinodally decomposed phase domains is strongly governed by the dynamics driven by the interfacial energy.[7] As shown in Figure 2, the well-defined co-continuous structure of the spinodal decomposition is a transient one, which coarsens self-similarly for a limited duration of time and then breaks up into fragments. To reduce the total interfacial energy, the system reorganizes the domain structure toward that with less interfacial area and less local interfacial energy.

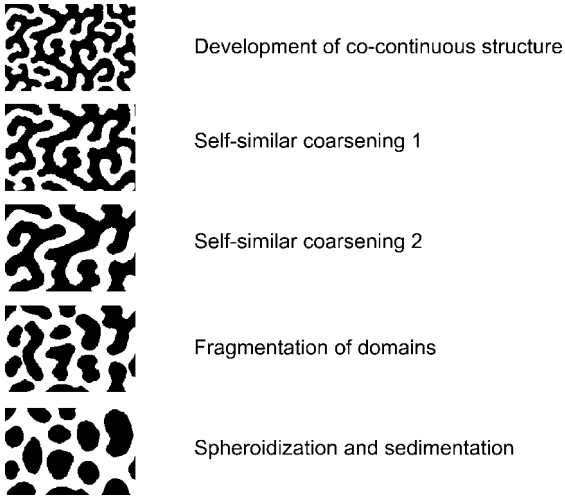

FIGURE 2. Time evolution of a spinodally decomposing isotropic symmetrical system.

Within the regime of self-similar coarsening (Figure 2, bottom), the geometrical features of the developing domains remain unchanged except the characteristic size. Then it is followed by the fragmentation of either of the continuous domains, which results in the dispersion of one phase within the other continuous phase.

Sol–gel transition is a dynamical freezing process that occurs via cross-linking reactions. If any transient (dynamic) heterogeneity is present in a gelling solution, it will be arrested in a gel network if the time scale of a sol–gel transition is short enough to take the "snapshot" of the transient heterogeneity. The "frozen" structure depends, therefore, on the onset of phase separation relative to the "freezing" point by sol–gel transition. The earlier the phase separation is initiated relative to the sol–gel transition, the coarser the resultant structure becomes, and vice versa. For example, a higher reaction temperature normally increases the mutual solubility of the constituents and hence suppresses the phase separation tendency, and in parallel, it accelerates the hydrolysis/polycondensation reactions. As a result, the onset of phase separation is retarded and the solution is solidified earlier by the sol–gel transition. Due to these duplicate effects, gels with drastically finer phase-separated domains are obtained at higher temperatures. With an appropriate choice of the reaction parameters such as starting composition and temperature, the pore size (domain size) and pore volume of the gels can be designed over a broad range.

3. Examples of Materials with Controlled Macropores

3.1. Pure Silica. As extensively listed in Table 2, pure silica formulations have been exploited to give every possible morphology, material shape, and doped composition. In the presence of a limited amount of water, using especially tetramethoxysilane (TMOS) as a precursor, the phase separation is induced just by adding polar solvent.[8] In the presence of a higher molar ratio of water to silicon, the phase separation is induced by polymeric or amphiphilic additives. Polymers or surfactants having no specific attractive interaction with silanol surfaces, e.g., poly(acrylic acid) or anionic polymers and surfactants, tend to be distributed to the "fluid phase" so that the amount of additives is directly related to the volume fraction of macropores. On the other hand, due to the strong hydrogen bonds between silanols and polyoxyethylenes, additives having -CH_2-CH_2-O- repeating units, poly(ethylene oxide) (PEO) and Pluronic or Brij families, are always distributed to the "gel phase", while the solvent mixture becomes a majority in the fluid phase. Similarly, cationic surfactants are preferentially distributed to the gel phase. In these cases, the volume fraction of the fluid phase can be controlled mostly by the amount of solvent, while the domain size is determined by the additive concentration which dominantly governs the phase separation tendency. This implies that one can independently design the volume and size of macropores by the concentrations of solvent and additive, respectively (Figure 3). For the gels prepared in a macroscopic mold followed by evaporation drying and heat treatment at 600 °C, the typical porosity (v/v) covers 40–80% with the median pore size ranging from 0.5 to 10 μm.[3] In addition, the strong attractive interaction between silica and additive molecule makes it possible to template the mesoscale structures of the structural unit of the gels by surfactants.

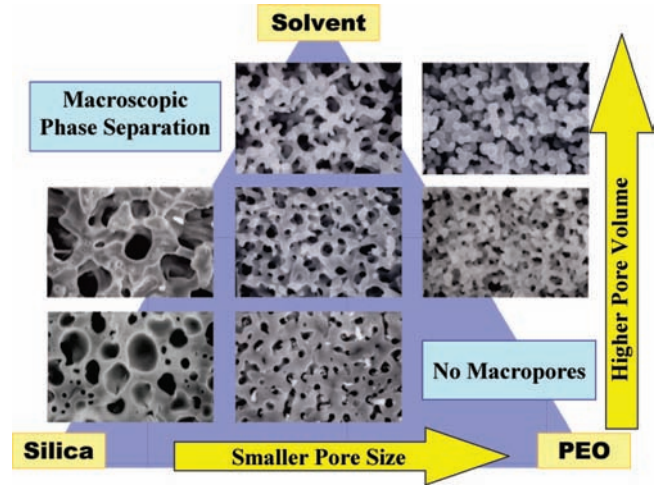

FIGURE 3. Schematic relations between starting composition and resultant gel morphologies in a pseudoternary [silica/poly(ethylene oxide)/solvent] system. Reproduced with permission from ref 24. Copyright 2001 American Chemical Society.

3.2. Siloxane-Based Organic–Inorganic Hybrids. Among the silicon alkoxides having trialkoxysilyl ligands, a clear distinction can be made between alkyltrialkoxysilanes, represented by methyltrimethoxysilane (MTMS) and bis(trialkoxysilyl)alkanes, represented by bis(trimethoxysilyl)ethane (BTME). Due to the strong tendency to form cyclic species in their polycondensation stage, gels obtained in a MTMS system often retain high density of methyl groups on the surface of the oligomers. On the other hand, gels prepared in a BTME system exhibit apparently higher surface hydrophilicity comparable to that of pure silica gels probably because ethylene bridges between the silicon atoms are buried in the network rather

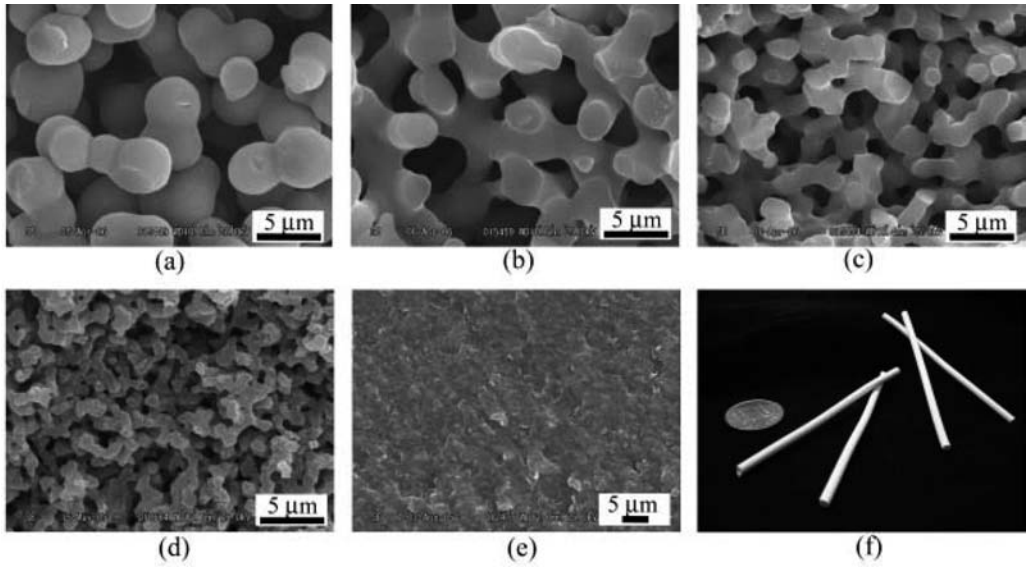

FIGURE 4. (a–e) SEM images of dried TiO_2 gels prepared with varied water/TiO_2 molar ratios in the overall starting 1:0.5:0.5:*f* Ti($O^nC_3H_7$)$_4$:HCl:formamide:water composition: (a) $f = 20.50$, (b) $f = 20.75$, (c) $f = 21.00$, (d) $f = 21.25$, and (e) $f = 21.50$. (f) Photo image of monolithic TiO_2 gels prepared in Teflon tubes and a coin. Reproduced with permission from ref 10. Copyright 2006 American Chemical Society.

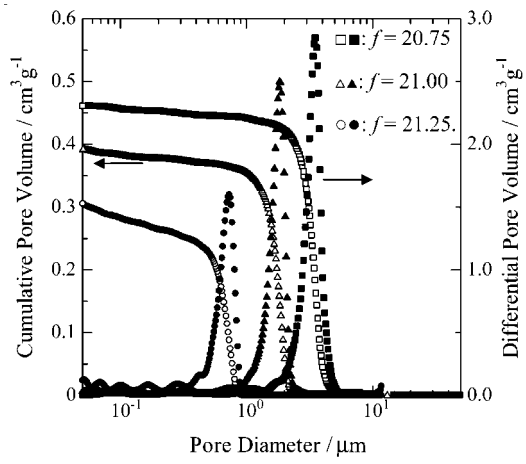

FIGURE 5. Pore size distribution of the dried TiO_2 gels measured by the mercury intrusion method: (□ and ■) $f = 20.75$, (▲ and △) $f = 21.00$, and (○ and ●) $f = 21.25$. Reproduced with permission from ref 10. Copyright 2006 American Chemical Society.

than exposed on the surface of the oligomers. It has also been experimentally confirmed that MTMS-derived oligomers phase-separate in a relatively less polar solvent composition; however, BTME hardly phase-separates even in highly polar solvent compositions.[9] Due to the presence of Si–C bonds, gels from both MTMS and BTME precursors exhibit much higher alkaline resistance than pure silica gels. Similar to the pure silica case, the BTME-derived gels with silanol-rich surfaces can be templated by surfactants to exhibit mesopores with well-defined size and shape.

3.3. Other Oxides. Alkoxides of titanium and zirconium generally exhibit much higher reactivity toward hydrolysis/polycondensation than those of silicon, mainly due to the difference in the partial charge of the metals in their respective oxygen-coordinated environments. Well-defined macroporous titania and zirconia have been very difficult to synthesize in monolithic form. Very recently, Konishi et al. reported that the use of titanium *n*-propoxide instead of *i*-propoxide at high concentrations of HCl enabled one to control the hydrolysis/polycondensation kinetics in an experimentally feasible time scale, where gelation occurs in a tens of minutes to a few hours.[10] The reaction can be well-controlled with a relatively limited amount of water against complete hydrolysis so that titania oligomers rich in unreacted alkoxy groups separate from a polar solvent mixture containing formamide. An appropriate amount of PEO can also be incorporated for an adjustment of phase separation dynamics to obtain better defined macroporous structures (Figures 4 and 5). Macroporous titania gels thus obtained are composed of a microcrystalline anatase phase even in the wet-gel stage. Via control of the grain growth of the anatase crystallites during the aging and heat treatment, the interstices of the crystallites form sharply distributed mesopores in the size range of 5–10 nm (Figure 6). Monolithic pure zirconia with controlled macropores can also be prepared with further care on synthesis. Zirconia tends to form gels with amorphous structural units and transforms via monoclinic into tetragonal as the heat treatment temperature increases. On the basis of the methods reported by Gash et al.,[11] the polymerization-induced phase separation has been successfully combined with the gel-forming reaction assisted by the ring-opening reaction of propylene oxide.[12] An addition of high-molecular mass (>100 kDa) PEO was found to be effective in slowing and precisely regulating the phase separation dynamics. The added PEO is mainly distributed to the fluid phase and has a minor effect on the mesopore formation. Macroporous morphologies and pore size distributions of α-alumina ceramics thus obtained are shown in Figure 7. On heat treatment, the monolithic gels transformed from amorphous via γ-alumina to α-alumina crystalline form without damage being done to the macroporous framework. Silica[13] and titania[14] gels with

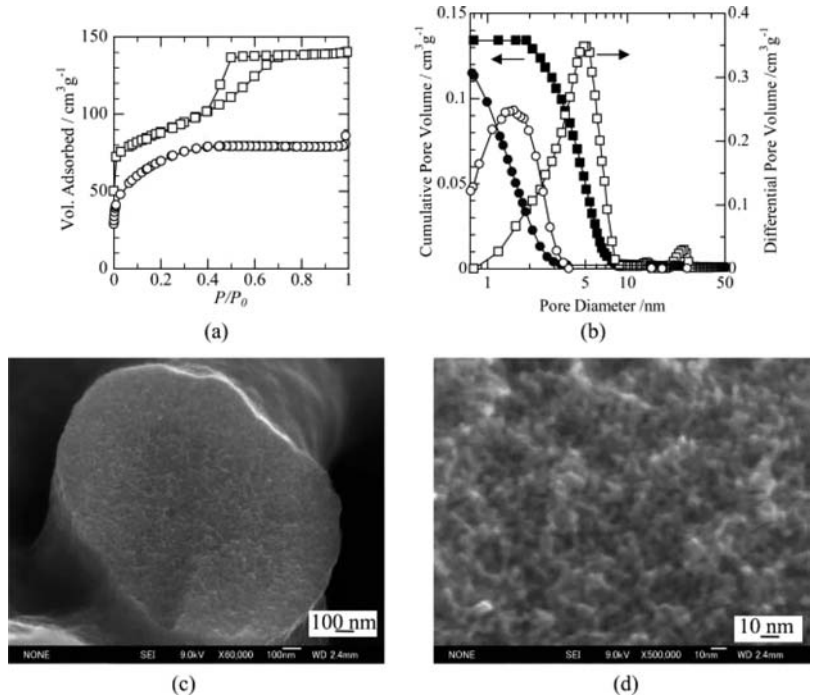

FIGURE 6. Mesoscale characterizations of the TiO_2 gels prepared with $f = 21.00$. (a) Nitrogen adsorption–desorption isotherms of the dried gel (○) and the gel heat-treated at 300 °C (□). The curve of the gel heat-treated at 300 °C is shifted upward by 50 cm^3/g for clarity. (b) Pore size distribution of the dried gel (○ and ●) and the gel heat-treated at 300 °C (□ and ■). (c) FE-SEM image of the gel heat-treated at 300 °C. (d) Higher-magnification image of panel c. Reproduced with permission from ref 10. Copyright 2006 American Chemical Society.

controlled macropores can also be prepared from colloidal dispersion of corresponding oxide particles with appropriate additives.

3.4. Characterization of Macropores. The three-dimensional observation of macropores and conjugate gel skeletons by laser scanning confocal microscopy (LSCM) has recently been developed. This method can improve the underestimation of the pore size by the conventional mercury intrusion often reported with networked pores. From the precise three-dimensional configurational information about the skeletons and pores, more detailed analysis of the interfacial morphology can be performed.[15] The technique has also been applied in the examination of anisotropic phase-separated skeleton structures in the vicinity of container walls[16] and in the determination of the macroporosity with higher accuracy to be correlated with the liquid flow behavior through monolithic gels.[17]

4. Tailoring Mesopores To Obtain Hierarchical Pore Structures

4.1. Post Gelation Aging of Oxide Gels. Since the interconnected macropores enhance the material transport within the bulk gel sample, the exchange of pore liquid with an external solvent can be performed much faster than for the case with gels having only meso- to micropores. Conventional methods of tailoring mesopore structure by aging wet silica gels under basic and/or hydrothermal conditions can be suitably applied to the monolithic macroporous silica gels without essentially disturbing the well-defined macroporous structure (Figure 8). Experimentally, the as-gelled wet monolithic specimen is immersed in an excess amount of an external solvent such as an aqueous ammonia solution. Alternatively, one can add urea in the starting composition of the gel preparation and subsequently heat the wet gel in a closed vessel to generate aqueous ammonia in situ. The preferential dissolution of gel network sites with small positive curvature and subsequent reprecipitation onto those with small negative curvature results in the reorganization of smaller pores into larger pores (the so called Ostwald ripening mechanism). In pure silica cases, the NMR and SAXS (small-angle X-ray scattering) measurements proved that the chemical reorganization of an initially microporous network into that with sharply distributed mesopores takes place on the time scale of a few hours.[18] It is noteworthy that the gel with much lower solubility in external aqueous solutions can also be treated under hydrothermal conditions to give enlarged and well-defined mesopore structures. Although the structural evolution under hydrothermal conditions is not known in detail, there may be a mechanism of structural reorganization by the cooperative motion of the network as a whole. In any case, these mesopore formation processes take place within the preformed micrometer-sized gel skeletons so that the size of mesopores can be controlled in a manner independent of the macropore size unless the local dissolution of the gel skeletons causes significant deformation of the whole macroporous framework during the solvent exchange.

4.2. Supramolecular Templating of Mesopores. The supramolecular templating is an attractive alternative to the postgelation aging process for obtaining mesopores with higher degrees of order in pore size, shape, and spatial arrangement. It has been found that several kinds

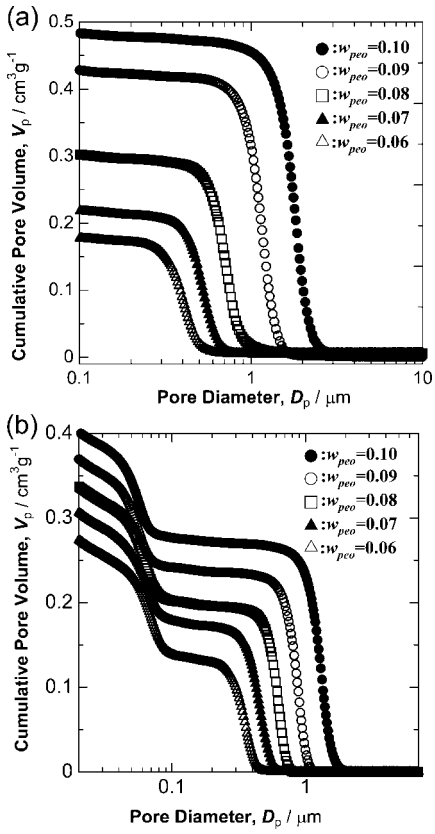

FIGURE 7. Pore size distribution of macroporous alumina prepared from aluminum chloride and before and after heat treatment at 1100 °C for 5 h. Starting composition: 2.16 g of $AlCl_3{\cdot}6H_2O$, 1.55 g of propylene oxide, 1.97 g of EtOH, 2.5 g of H_2O, and w_{PEO} g of PEO.

of surfactants can be used to induce the phase separation concurrently with the sol–gel transition.[19–21] With an appropriate choice of surfactants suitable also for the supramolecular templating of mesopores, materials have been prepared with crystal-like long-range ordered mesopores homogeneously located in the micrometer-sized well-defined gel skeletons.

The key to combining phase separation and gelation with supramolecular templating and precipitation is that both processes include a kind of polymerization-induced phase separation. It has been established that cooperative assembly between surfactant micelles and oligomeric oxides enhances the ordered arrangement of the micelles. Highly ordered mesostructures are organized by such a cooperative assembly mechanism in generally amorphous oxide networks. Due to relatively strong attractive interactions between micelles and oxides, submicrometer- to micrometer-sized particles are precipitated out of the solution in dilute systems under a closed condition.

Starting from a composition favorable for the formation of co-continuous macroporous structure containing a triblock copolymer Pluronic P123 (EO_{20}–PO_{70}–EO_{20}; EO, ethylene oxide; PO, propylene oxide), we introduced an additive, 1,3,5-trimethylbenzene (TMB), known to preferentially be distributed to the hydrophobic cores of micelles, to enhance long-range ordering of mesophases in both BTME[22] and TMOS-derived[23] systems. Alternatively, a large amount of water together with a high

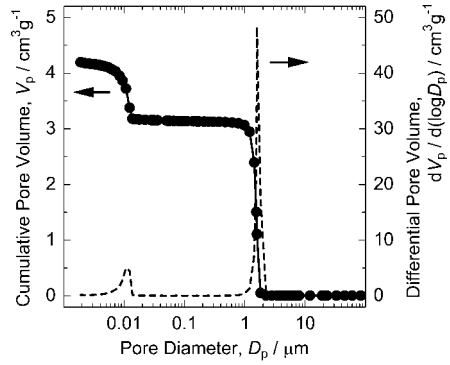

FIGURE 8. Pore size distribution of porous silica with hierarchical meso- and macropores optimized for monolithic HPLC columns. Reproduced with permission from ref 3. Copyright 1997 Springer.

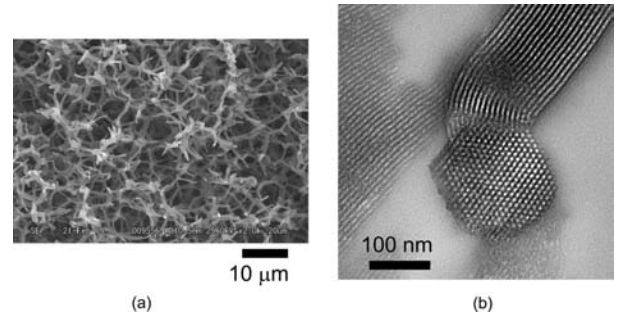

FIGURE 9. SEM and TEM photographs of a heat-treated gel sample with highly ordered two-dimensional hexagonal mesopores.

concentration of P123 was used. In heat-treated gels, the long-range ordering of cylindrical pores in two-dimensional hexagonal symmetry has been confirmed by XRD measurements that indicate sharp peaks comparable to single-crystal-like SBA-15.[23] Further, the real-space observations have been performed by SEM and TEM (Figure 9). It is noteworthy that the shape of gel skeletons is affected by the anisotropy of mesopores contained in the skeletons; that is, those with cylindrical mesopores exhibit fibrous features.

5. Applications and Products

5.1. Monolithic Silica HPLC Columns. One major area of application for hierarchically porous pure silica materials is liquid chromatography (LC) as a column packing material. Monolithic silica columns having co-continuous structures can provide better total performance than conventional columns packed with particles that have been used for LC for more than 100 years.[24–26] The thin skeletons lead to high efficiency based on fast equilibration of solutes between a mobile liquid phase and a stationary solid phase on the mesopore walls, while the large macropores contribute to high permeability. In this section, the highest-performance monolithic silica columns and their future possibilities will be discussed.

In LC, the efficiency (N, a number of theoretical plates) of a column (length L) is given by eq 2,[27] where H stands for a plate height and σ^2 a variance of a Gaussian-shaped solute band the solute acquires during the migration through the column. N is usually calculated from retention

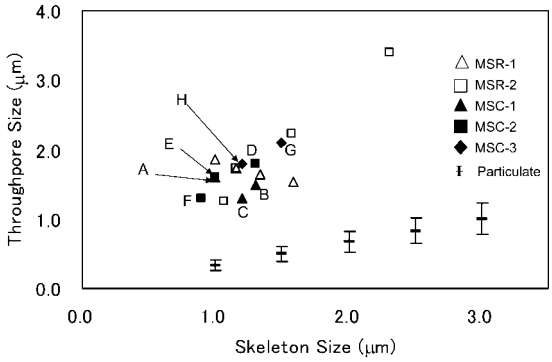

FIGURE 10. Plots of through-pore size against skeleton size for monolithic silica columns.

time of a solute (t_R) and the base peak width ($t_W = 4\sigma$; σ, standard deviation).

$$N = L^2/\sigma^2 = 16t_R/t_W \quad (2a)$$

$$H = \sigma^2/L = L/N \quad (2b)$$

Plate height H is dependent on particle size (d_p) and mobile phase linear velocity (u) as shown in eq 3, where C_E, C_D, and C_S are the coefficients indicating the contributions of the eddy diffusion, molecular diffusion, and slow mass transfer to band broadening, respectively. The smaller d_p gives the higher efficiency by the faster mass transfer based on the shorter diffusion path length inside and outside the particles, whereas the small d_p causes a large pressure drop due to the small interstitial flow paths (eq 4; η, solvent viscosity), where ϕ (a flow resistance factor) is commonly 700–1000 for a particle-packed column.[28]

$$H = C_E d_p + C_D/u + C_S d_p u \quad (3)$$

$$\Delta P = \phi \eta u L / {d_p}^2 \quad (4)$$

High efficiency (large N) and low pressure (small ΔP) are desirable for high resolution and high speed. Separation time is dictated by L, and the smaller d_p allows the use of a shorter column. Actually, H is approximately $2d_p$ at optimum linear velocity. Recently 1.7–2 μm particles have started to provide greatly enhanced N per unit time[29,30] compared to conventional 3–5 μm particles, although accompanied by high pressure in proportion to $1/{d_p}^2$. Their optimum performance can be obtained with a specially designed instrument. Common HPLC equipment possesses a 35–40 MPa pressure limit.

Monolithic silica columns having co-continuous structures can simultaneously provide higher column efficiency and lower pressure than a particle-packed column.[24–26] Figure 10 shows the plot of the through-pore size against the size of the silica skeleton for monolithic silica columns prepared in a test tube (MSR)[31,32] or in a capillary (MSC).[33,34] Through-pore size/skeleton size ratios in the range of 1–2 have been obtained for all the monolithic silica columns that are much larger than those of particle-packed columns at 0.25–0.4 (the range indicated as bars in Figure 10).[35] The particle size dictates the size of interstitial voids for particle-packed columns, while the structures can be designed for monolithic columns.

Table 3. Composition of the Feed Mixtures for the Preparation of Monolithic Silica Columns in a 100 μm Capillary, MS(100), and Size of Domains and Silica Skeletons of the Products[34]

column (symbol in Figure *10*)	TMOS[a] (mL)	PEG[a] (g)	domain size (μm)	skeleton size (μm)
MS(100)-G[b]	40	12.4	3.6	1.5
MS(100)-A[c]	56	11.8	2.6	1.0
MS(100)-B[c]	64	10.4	2.8	1.3
MS(100)-C[c]	72	8.4	2.5	1.2
MS(100)-H[b]	40	12.8	3.0	1.2
MS(100)-D[c]	56	11.7	3.1	1.3
MS(100)-E[c]	56	11.8	2.6	1.0
MS(100)-F[c]	56	11.9	2.2	0.9

[a] The amount of TMOS and PEG used with urea (9.0 g) and CH_3COOH (100 mL). PEG, polyethylene glycol, chemically equivalent to PEO with terminal OH groups. [b] Prepared at 30 °C. [c] At 25 °C.

Commercially available MSR columns (4.6 mm diameter, 1–10 cm length) clad with PEEK resin, possessing 2 μm through-pores, 1–1.5 μm skeletons, and a relatively wide distribution of mesopores around 13 nm[36] result in a back pressure equivalent to that of 7–10 μm particles and an efficiency equivalent to that of 3.5–4 μm particles.[37,38] Performance better than that of commonly used 5 μm particles in either respect is made possible by the large-sized through-pores and the small-sized skeletons. The column efficiency, however, was much lower than expected from the skeleton size, presumably due to the presence of large through-pores. Similar results have been obtained for monolithic silica capillary columns.[33] The porosity and through-pore size of monolithic silica prepared in a capillary tend to be large, because the silica must be covalently attached to the capillary wall to prevent shrinkage of the whole structure. It is necessary to reduce the size of through-pores and skeletons of monolithic silica to achieve similar or higher efficiency compared to that of the most advanced particles of 1.7–2 μm.

In a series of experiment, the columns listed in Table 3 were prepared from TMOS.[34] Columns MS(100)-A–C (a group of columns, MSC-1, in Figure 10) were prepared in an effort to examine the effect of the porosity, or the effect of the TMOS concentration in the feed on the structure and performance. The reaction was carried out with adjusted poly(ethylene glycol) (PEG) concentrations to synchronize phase separation and gelation. The lower reaction temperature slowed the polymerization which resulted in slower phase separation and gelation. The higher TMOS concentrations cause the faster gelation, while the increased PEG concentrations result in the slower phase separation. Similarly, columns MS(100)-D–F (MSC-2) were prepared with the varied PEG concentrations in an effort to examine the effect of domain size on column efficiency at constant porosity. Along with each series, columns G and H were prepared with lower TMOS concentrations as in a previous study[33] that resulted in inhomogeneous aggregated skeletons, as shown in Figure 11a.[34] Figure 10 indicates that an increase in the TMOS concentration resulted in the larger skeleton size and smaller through-pore size, as expected (MSR-1 and MSC-

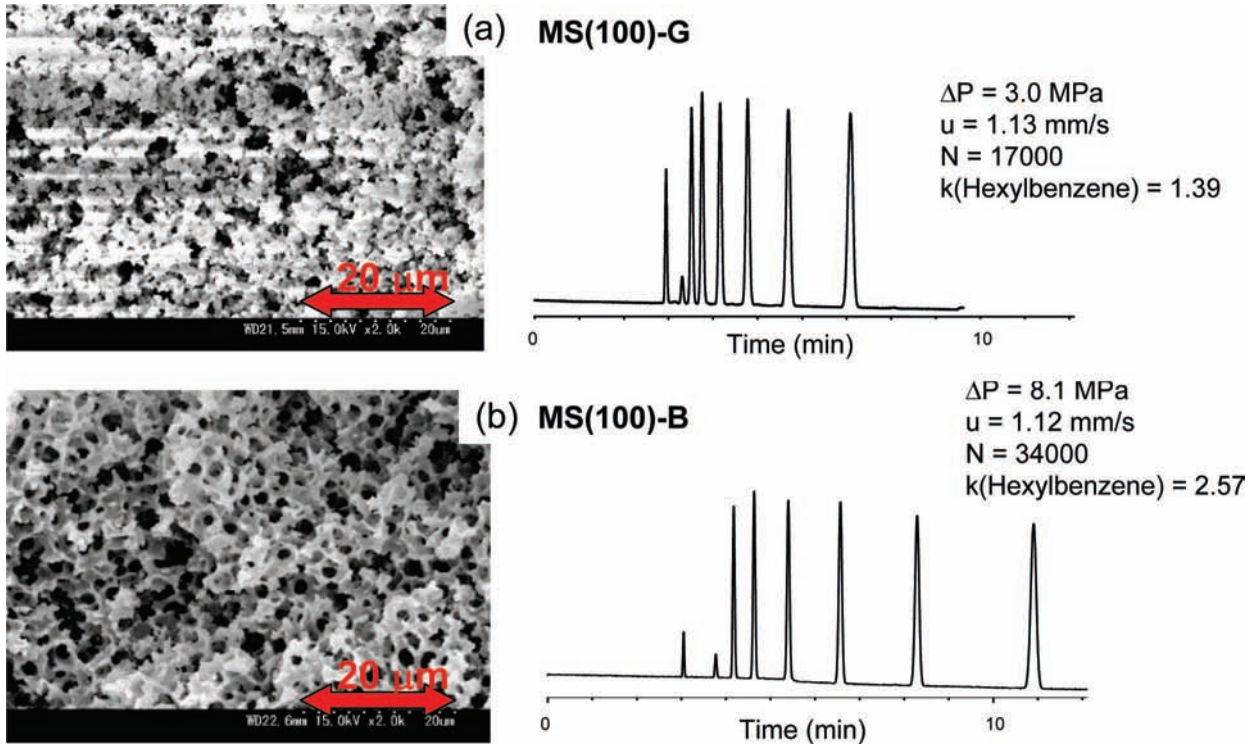

FIGURE 11. SEM images and chromatograms obtained for monolithic silica capillary columns.[34] Chromatograms were obtained for uracil (the first peak) and alkylbenzenes [$C_6H_5(CH_2)_nH$, where n = 0–6]. Column: (a) MS(100)-G and (b) MS(100)-B, 100 μm inside diameter and 25 cm long (effective length of 20 cm). Mobile phase: 80:20 methanol/water. Temperature: 30 °C. Reproduced with permission from ref 34. Copyright 2006 American Chemical Society.

1). With a fixed amount of TMOS, an increase in the amount of PEG resulted in a decrease in domain size with almost constant through-pore size/skeleton size ratios (MSR-2, MSC-2, and MSC-3).

As shown in Figure 11, MS(100)-B (as well as columns A and C) prepared at 25 °C with reduced porosity possesses a much higher homogeneity of co-continuous structures and resulted in a much higher N than MS(100)-G prepared at 30 °C. Since the structural inhomogeneity is expected to result from the disturbed coarsening process of the phase-separating domains, the lower temperature contributed to the suppression of the coarsening via the increased viscosity of the whole system. It has been predicted that a decrease in porosity and an increase in homogeneity would improve the performance of monolithic columns.[39] Actually, all columns (A–F) prepared at a lower temperature and with a lower porosity were shown to possess much higher homogeneity than columns G and H. For columns D–F, the increase in PEG concentration in feed resulted in the smaller domain size. The increase in a skeleton volume, or the increase in the TMOS content in the feed, is reflected in the greater solute retention observed for columns A–F than for G or H, as shown in Figure 11.

Column F, having the smallest domain size, exhibited a slightly higher column efficiency, N, than column D or E by 5–10%. The total performance, $(N/t_0)(N/\Delta P)$ (t_0, a column dead time), of column F, however, was found to be lower than that of column D by ca. 30%, implying that optimum reaction conditions for each TMOS concentration are very narrow. In other words, one set of feed compositions with a change in the concentration of one component could not produce a wide range of monolithic structures with desirable homogeneity. The adverse effects of inhomogeneous structures are reported to be pronounced at the smaller domain sizes.[40] In fact, monolithic silica columns A, B, and D–F were shown to provide faster separations than any particle-packed column for a region of N greater than ca. 25 000.[34] The greatest advantage of a monolithic column such as columns D–F is that the efficiency of 2–2.5 μm particles can be obtained with a pressure drop of 5–6 μm particles. Figure 10 also suggests that performance equivalent to that of 1.5 μm particles can be expected somewhere around 1 μm through-pore size and 0.8 μm skeleton size.

The use of a long monolithic silica capillary column is an easy and viable approach to increasing the number of separated peaks per unit time. (It is difficult to pack a long capillary column with small-sized particles.) In a LC–mass spectrometry (MS) system, the use of a monolithic silica capillary column resulted in better resolution by LC and the detection and identification of a greater number of peaks by MS. Figure 12 shows a comparison of chromatograms for the gradient elution of methanol extracts of *Arabidopsis thaliana* leaf using 30–90 cm monolithic silica capillary columns.[41] The major factor for the improved resolution and detection of the cell content is the increase in column efficiency with the increased column length, resulting in a reduction in the extent of ion suppression. It is known that the less easily ionizable solutes in an unresolved solute band tend to be suppressed from ionization. The small amounts of sample and mobile

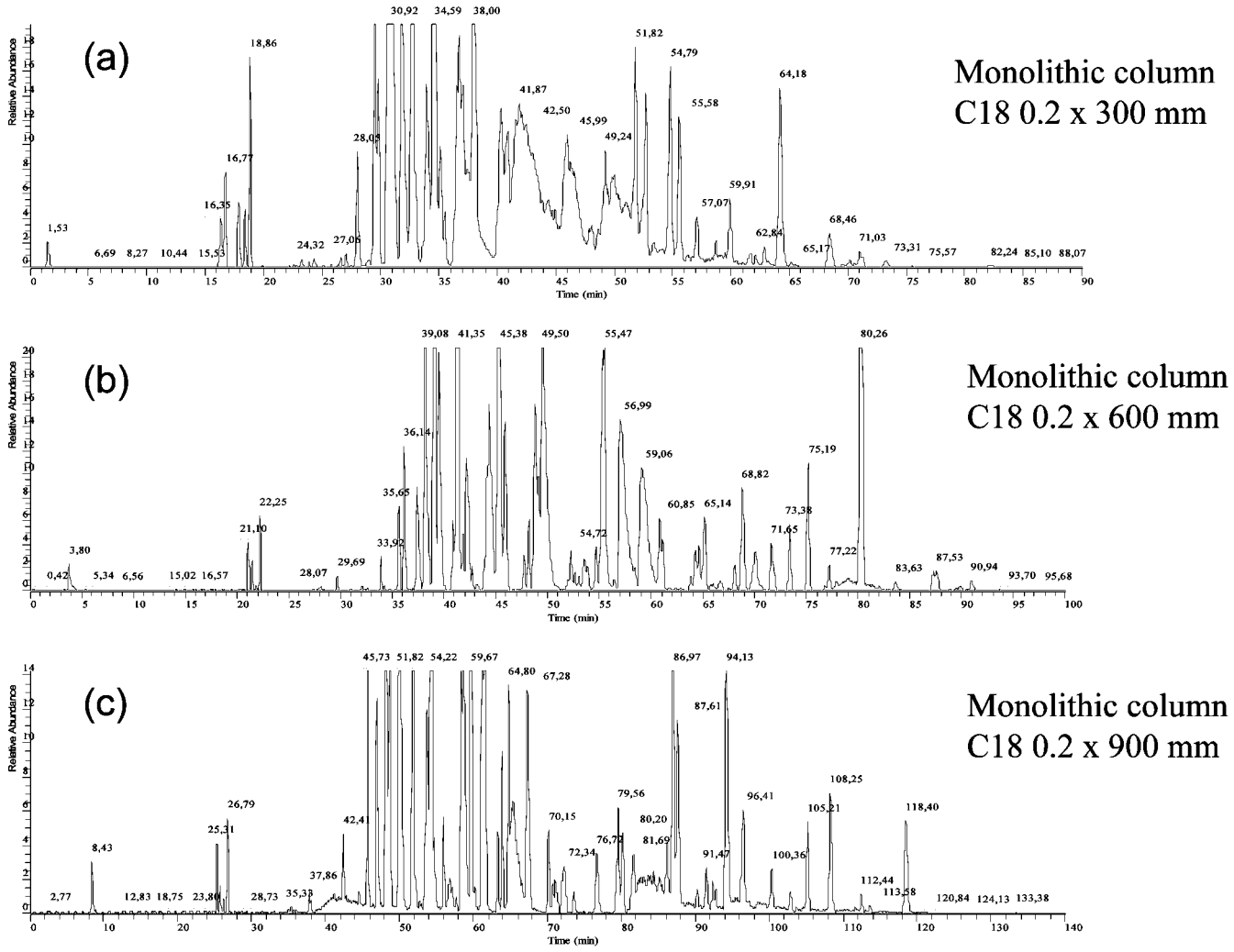

FIGURE 12. Replicate injections of an *Arabidopsis* leaf methanol extract on capillary monolithic C_{18} columns in positive ionization full-scan MS, given as base peak chromatograms. Column: (a) 0.2 mm × 300 mm, (b) 0.2 mm × 600 mm, and (c) 0.2 mm × 900 mm. Mobile phase A, 6.5 mM ammonium acetate (pH 5.5, adjusted by acetic acid); moblie phase B, acetonitrile. Cycle: (a) from 5 to 20% B from 0 to 15 min, to 70% B from 15 to 22 min, and to 100% B from 22 to 57 min, at 2.6 mm/s; (b) from 5 to 20% B from 0 to 15 min, to 70% B from 15 to 23 min, to 100% B from 23 to 75 min, at 2.6 mm/s; and (c) from 5 to 20% B from 0 to 16 min, to 70% B from 16 to 23 min, to 100% B from 23 to 110 min, at 1.8 mm/s. Reproduced with permission from ref 41. Copyright 2003 American Chemical Society.

phase required in addition to compatibility with a nano-electrospray ionization interface are features of capillary HPLC. It was possible to detect 200 components by using software for the separation shown in Figure 12c. The extremely high separation capability was also shown very nicely in a proteomic study using a 20 μm inside diameter, 70 cm monolithic silica capillary column providing a peak capacity of 420 in 210 min.[42]

The generation of ultrahigh efficiency by long capillary format[41,42] will need high extraskeleton porosity (ca. 0.7 or above),[39] while high-speed separations with an N of 10000–30000 need small-sized domains and the lower porosity (ca. 0.4–0.6).[34,39] The development of monolithic silica columns having controlled domain size and porosity, and most importantly high homogeneity, will be crucial for high-speed and high-efficiency LC separations in the future, if one recognizes the advantages of monolithic columns over conventional particulate columns. The preparation of these materials for LC requires preparation conditions more rigorously controlled than those of common sol–gel products. Optimum reaction conditions can be found in a narrow range of concentrations of each component. Chromatography is such a delicate means of testing the size and homogeneity of co-continuous structures. Facile preparation of polar-modified surfaces[43] and stability against high flow rate required for multidimensional applications[44] make monolithic silica even more attractive, in spite of the disadvantages related to the silica preparation and the chemical modification in individual columns.

5.2. Future Challenges and Additional Applications. Monolithic materials with highly controlled inner surfaces such as well-defined hierarchical pores can be used in many of the areas where the particle-packed structure has been playing an important role. The low liquid-flow resistance (high permeability) and enhanced accessibility to the nanoscale surfaces of monolithic hierarchically porous materials are advantageous to every reaction/separation/purification process. However, for the full utilization of the potential of monolithic columns, further

improvement in the structural homogeneity on the submicrometer length scale is needed.

Liquid-phase catalytic reactions can be enhanced in a device composed of immobilized enzyme or catalyst in general.[45] Kato et al.[46] recently prepared a flow-through bio-reactor made of a macroporous silica monolith support incorporated with immobilized trypsin. The pipette tip-type device for rapid digestion by trypsin has also been reported. Similarly, materials for solid-phase extraction (SPE) purposes can be easily designed to exhibit superior permeability and extraction efficiency.[47–49]

After the establishment of pure silica, the chemical compositions have been continuously extended to various pure oxides and complex oxides, organic–inorganic hybrids, and even fully organic polymers.[50] Depending on the field of application, the appropriate chemical composition can be tuned in terms of mechanical and chemical stability as well as surface chemistries.

6. Conclusions

Polymerization-induced phase separation in oxide sol–gel systems is unique in that a wide variety of transient multiphase structures are frozen in the gelled samples. Recent success in inducing concurrent phase separation and sol–gel transition in many oxide systems and from various types of precursors implies that the phenomenon is independent of the mechanism of gelation (chemical polymerization or physical aggregation). The very essential requirement is simply "competitive" phase separation and sol–gel transition both in length scale and in time scale.

With an extension of the material shape and size, the effect of spatial confinement on the structure development becomes significant. A deeper understanding is still needed to completely control the morphology, especially in the miniaturized spaces. Further development of chemical modification of the pore surfaces as well as impregnating functional molecules will enhance the application of the well-defined hierarchically porous material. Continuous efforts are being made to integrate a wide variety of highly ordered mesophases into well-defined assemblies in longer length scales with extended chemical compositions.

We thank Dr. Hiroyoshi Minakuchi at Kyoto Monotech Corp. The contribution of Prof. Hiroshi Jinnai (Kyoto Institute of Technology) to TEM observation is sincerely acknowledged. This work was partly supported by a Grant for Practical Application of University R&D Results under the Matching Fund Method from the New Energy and Industrial Technology Development Organization (NEDO), Japan.

References

(1) (a) Nakanishi, K.; Soga, N. Phase Separation in Gelling Silica-Organic Polymer Solution: Systems Containing Poly(sodium styrenesulfonate). *J. Am. Ceram. Soc.* **1991**, *74*, 2518–2530. (b) Nakanishi, K.; Soga, N. Phase separation in silica sol-gel system containing polyacrylic acid I. Gel formation behavior and effect of solvent composition. *J. Non-Cryst. Solids* **1992**, *139*, 1–13.

(2) Nordberg, M. E. Properties of some Vycor-brand glasses. *J. Am. Ceram. Soc.* **1944**, *27*, 299–304.

(3) Nakanishi, K. Pore Structure Control of Silica Gels Based on Phase Separation. *J. Porous Mater.* **1997**, *4*, 67–112.

(4) Brinker, C. J.; Scherer, G. W. *Sol-Gel Science: The Physics and Chemistry of Sol-Gel Processing*; Academic Press: New York, 1990; pp 108–216.

(5) Flory, P. J. *Principles of Polymer Chemistry*; Cornell University Press: Ithaca, NY, 1971.

(6) deGennes, P. G. *Scaling Concepts in Polymer Physics*; Cornell University Press: Ithaca, NY, 1979; p 73.

(7) Hashimoto, T.; Itakura, M.; Hasegawa, H. Late stage spinodal decomposition of a binary polymer mixture. I. Critical test of dynamical scaling on scattering function. *J. Chem. Phys.* **1986**, *85*, 6118–6128.

(8) Kaji, H.; Nakanishi, K.; Soga, N. Polymerization-induced phase separation in silica sol-gel systems containing formamide. *J. Sol-Gel Sci. Technol.* **1993**, *1*, 35–46.

(9) (a) Nakanishi, K.; Yamato, T.; Hirao, K. Phase Separation in Alkylene-Bridged Polysilsesquioxane Sol-Gel Systems. *Mater. Res. Soc. Symp. Proc.* **2002**, *726*, Q9.7.1-6. (b) Nakanishi, K.; Kanamori, K. Organic-inorganic hybrid polysilsesquioxane monoliths with controlled macro- and mesopores. *J. Mater. Chem.* **2005**, *15*, 3776–3786.

(10) Konishi, J.; Fujita, K.; Nakanishi, K.; Hirao, K. Monolithic TiO_2 with Controlled Multiscale Porosity via a Template-Free Sol-Gel Process Accompanied by Phase Separation. *Chem. Mater.* **2006**, *18*, 6069–6074.

(11) Gash, A. E.; Tillotson, T. M.; Satcher, J. H., Jr.; Poco, J. F.; Hrubesh, L. W.; Simpson, R. L. Use of Epoxides in the Sol-Gel Synthesis of Porous Iron(III) Oxide Monoliths from Fe(III) Salts. *Chem. Mater.* **2001**, *13*, 999–1007.

(12) Tokudome, Y.; Fujta, K.; Nakanishi, K.; Miura, K.; Hirao, K. Synthesis of Monolithic Al_2O_3 with Well-Defined Macropores and Mesostructured Skeletons via the Sol-Gel Process Accompanied by Phase Separation. *Chem. Mater.* **2007,** doi 10.1021/cm063051p.

(13) (a) Shoup, R. D. Controlled Pore Silica Bodies Gelled From Silica Sol-Alkali Silicate Mixtures. In *Colloid and Interface Science*; Kerker, M., Ed.; Academic Press: New York, 1976; Vol. *3*, p 63. (b) Takahashi, R.; Sato, S.; Sodesawa, T.; Azuma, T. Silica with Bimodal Pores for Solid Catalysts Prepared from Water Glass. *J. Sol-Gel Sci. Technol.* **2004**, *31*, 373–376.

(14) Konishi, J.; Fujita, K.; Nakanishi, K.; Hirao, K. Phase-Separation-Induced Titania Monoliths with Well-Defined Macropores and Mesostructured Framework from Colloid-Derived Sol-Gel Systems. *Chem. Mater.* **2006**, *18*, 864–866.

(15) Jinnai, H.; Nakanishi, K.; Nishikawa, Y.; Yamanaka, J.; Hashimoto, T. Three-Dimensional Structure of a Sintered Macroporous Silica Gel. *Langmuir* **2001**, *17*, 619–625.

(16) Kanamori, K.; Nakanishi, K.; Hirao, K.; Jinnai, H. Three-Dimensional Observation of Phase-Separated Silica-Based Gels Confined between Parallel Plates. *Langmuir* **2003**, *19*, 5581–5585.

(17) Saito, H.; Nakanishi, K.; Hirao, K.; Jinnai, H. Mutual consistency between simulated and measured pressure drops in silica monoliths based on geometrical parameters obtained by three-dimensional laser scanning confocal microscope observations. *J. Chromatogr., A* **2006**, *1119*, 95–104.

(18) Nakanishi, K.; Takahashi, R.; Nagakane, T.; Kitayama, K.; Koheiya, N.; Shikata, H.; Soga, N. Formation of Hierarchical Pore Structure in Silica Gel. *J. Sol-Gel Sci. Technol.* **2000**, *17*, 191–210.

(19) Nakanishi, K.; Nagakane, T.; Soga, N. Designing Double Pore Structure in Alkoxy-Derived Silica Incorporated with Nonionic Surfactant. *J. Porous Mater.* **1998**, *5*, 103–110.

(20) Sato, Y.; Nakanishi, K.; Hirao, K.; Jinnai, H.; Shibayama, M.; Melnichenko, Y. B.; Wignall, G. D. Formation of ordered macropores and templated nanopores in silica sol-gel system incorporated with EO-PO-EO triblock copolymer. *Colloids Surf., A* **2001**, *187/188*, 117–122.

(21) Nakanishi, K.; Sato, Y.; Ruyat, Y.; Hirao, K. Supramolecular Templating of Mesopores in Phase-Separating Silica Sol-Gels Incorporated with Cationic Surfactant. *J. Sol-Gel Sci. Technol.* **2003**, *26*, 567–570.

(22) Nakanishi, K.; Kobayashi, Y.; Amatani, T.; Hirao, K.; Kodaira, T. Spontaneous Formation of Hierarchical Macro-Mesoporous Ethane-Silica Monolith. *Chem. Mater.* **2004**, *16*, 3652–3658.

(23) Amatani, T.; Nakanishi, K.; Hirao, K.; Kodaira, T. Monolithic Periodic Mesoporous Silica with Well-Defined Macropores. *Chem. Mater.* **2005**, *17*, 2114–2119.

(24) Tanaka, N.; Kobayashi, H.; Nakanishi, K.; Minakuchi, H.; Ishizuka, N. Monolithic LC Columns. *Anal. Chem.* **2001**, *73*, 420A–429A.

(25) Cabrera, K. Applications of silica-based monolithic HPLC columns. *J. Sep. Sci.* **2004**, *27*, 843–852.

(26) Kobayashi, H.; Ikegami, T.; Kimura, H.; Hara, T.; Tokuda, D.; Tanaka, N. Properties of Monolithic Silica Columns for HPLC. *Anal. Sci.* **2006**, *22*, 491–501.

(27) Giddings, J. C. *Unified Separation Science*; Wiley: New York, 1991; Chapter 5, p 101.
(28) Bristow, P. A.; Knox, J. H. Standardization of test conditions for high performance liquid chromatography columns. *Chromatographia* **1977**, *10*, 279–289.
(29) Gilar, M.; Daly, A. E.; Kele, M.; Neue, U. D.; Gebler, J. C. Implications of column peak capacity on the separation of complex peptide mixtures in single- and two-dimensional high-performance liquid chromatography. *J. Chromatogr., A* **2004**, *1061*, 183–192.
(30) Mellors, J. S.; Jorgenson, J. W. Use of 1.5 μm Porous Ethyl-Bridged Hybrid Particles as a Stationary-Phase Support for Reversed-Phase Ultrahigh-Pressure Liquid Chromatography. *Anal. Chem.* **2004**, *76*, 5441–5450.
(31) Minakuchi, H.; Nakanishi, K.; Soga, N.; Ishizuka, N.; Tanaka, N. Effect of skeleton size on the performance of octadecylsilylated continuous porous silica columns in reversed-phase liquid chromatography. *J. Chromatogr., A* **1997**, *762*, 135–146.
(32) Minakuchi, H.; Nakanishi, K.; Soga, N.; Ishizuka, N.; Tanaka, N. Effect of domain size on the performance of octadecylsilylated continuous porous silica columns in reversed-phase liquid chromatography. *J. Chromatogr., A* **1998**, *797*, 121–131.
(33) Motokawa, M.; Kobayashi, H.; Ishizuka, N.; Minakuchi, H.; Nakanishi, K.; Jinnai, H.; Hosoya, K.; Ikegami, T.; Tanaka, N. Monolithic silica columns with various skeleton sizes and through-pore sizes for capillary liquid chromatography. *J. Chromatogr., A* **2002**, *961*, 53–63.
(34) Hara, T.; Kobayashi, H.; Ikegami, T.; Nakanishi, K.; Tanaka, N. Performance of Monolithic Silica Capillary Columns with Increased Phase Ratios and Small-Sized Domains. *Anal. Chem.* **2006**, *78*, 7632–7642.
(35) Unger, K. K. Porous Silica. *Journal of Chromatography Library*; Elsevier: Amsterdam, 1979; Vol. *16*, Chapter 5.
(36) Al-Bokari, M.; Cherrak, D.; Guiochon, G. Determination of the porosities of monolithic columns by inverse size-exclusion chromatography. *J. Chromatogr., A* **2002**, *975*, 275–284.
(37) Miyabe, K.; Cavazzini, A.; Gritti, F.; Kele, M.; Guiochon, G. Moment Analysis of Mass-Transfer Kinetics in C_{18}-Silica Monolithic Columns. *Anal. Chem.* **2003**, *75*, 6975–6986.
(38) Leinweber, F. C.; Tallarek, U. Chromatographic performance of monolithic and particulate stationary phases: Hydrodynamics and adsorption capacity. *J. Chromatogr., A* **2003**, *1006*, 207–228.
(39) Gzil, P.; Vervoort, N.; Baron, G. V.; Desmet, G. General Rules for the Optimal External Porosity of LC Supports. *Anal. Chem.* **2004**, *76*, 6707–6718.
(40) Billen, J.; Gzil, P.; Desmet, G. Domain Size-Induced Heterogeneity as Performance Limitation of Small-Domain Monolithic Columns and Other LC Support Types. *Anal. Chem.* **2006**, *78*, 6191–6201.
(41) Tolstikov, V. V.; Lommen, A.; Nakanishi, K.; Tanaka, N.; Fiehn, O. Monolithic Silica-Based Capillary Reversed-Phase Liquid Chromatography/Electrospray Mass Spectrometry for Plant Metabolomics. *Anal. Chem.* **2003**, *75*, 6737–6740.
(42) Luo, Q. Z.; Shen, Y. F.; Hixson, K. K.; Zhao, R.; Yang, F.; Moore, R. J.; Mottaz, H. M.; Smith, R. D. Preparation of 20 μm-i.d. Silica-Based Monolithic Columns and Their Performance for Proteomics Analyses. *Anal. Chem.* **2005**, *77*, 5028–5035.
(43) Ikegami, T.; Horie, K.; Jaafar, J.; Hosoya, K.; Tanaka, N. Preparation of highly efficient monolithic silica capillary columns for the separations in weak cation-exchange and HILIC modes. *J. Biochem. Biophys. Methods* **2007**, *70*, 31–37.
(44) Tanaka, N.; Kimura, H.; Tokuda, D.; Hosoya, K.; Ikegami, T.; Ishizuka, N.; Minakuchi, H.; Nakanishi, K.; Shintani, Y.; Furuno, M.; Cabrera, K. Simple and Comprehensive Two-Dimensional Reversed-Phase HPLC Using Monolithic Silica Columns. *Anal. Chem.* **2004**, *76*, 1273–1281.
(45) Takahashi, R.; Sato, S.; Sodesawa, T.; Arai, K.; Yabuki, M. Effect of diffusion in catalytic dehydration of alcohol over silica-alumina with continuous macropores. *J. Catal.* **2005**, *229*, 24–29.
(46) Kato, M.; Inuzuka, K.; Sakai-Kato, K.; Toyo'oka, K. Monolithic Bioreactor Immobilizing Trypsin for High-Throughput Analysis. *Anal. Chem.* **2005**, *77*, 1813–1818.
(47) Shintani, Y.; Zhou, X.; Furuno, M.; Minakuchi, H.; Nakanishi, K. Monolithic silica column for in-tube solid-phase microextraction coupled to high-performance liquid chromatography. *J. Chromatogr., A* **2003**, *985*, 351–357.
(48) Miyazaki, S.; Morisato, K.; Ishizuka, N.; Minakuchi, H.; Shintani, Y.; Furuno, M.; Nakanishi, K. Development of a monolithic silica extraction tip for the analysis of proteins. *J. Chromatogr., A* **2004**, *1043*, 19–25.
(49) Ota, S.; Miyazaki, S.; Matsuoka, H.; Morisato, K.; Shintani, Y.; Nakanishi, K. High-throughput protein digestion by trypsin-immobilized monolithic silica with pipette-tip formula. *J. Biochem. Biophys. Methods* **2007**, in press.
(50) Kanamori, K.; Nakanishi, K.; Hanada, T. Rigid Macroporous Poly(divinylbenzene) Monoliths with a Well-Defined Bicontinuous Morphology Prepared by Living Radical Polymerization. *Adv. Mater.* **2006**, *18*, 2407–2411.

AR600034P